

Article

Mobility and Bioavailability of Metal(loid)s in a Fluvial System Affected by the Mining and Industrial Processing of Pb

Unai Cortada ^{1,2} , María Carmen Hidalgo ^{1,*} , Julián Martínez ³  and María José de la Torre ¹

¹ Department of Geology, EPSL and CEACTEMA, Scientific and Technological Campus, University of Jaen, 23700 Linares, Spain; ucortada@ujaen.es (U.C.); mjtorre@ujaen.es (M.J.d.l.T.)

² AFESA Medio Ambiente, S.A., Ed. San Isidro II, Idorsolo Kalea, 15, 48160 Bizkaia, Spain

³ Department of Mechanical and Mining Engineering, EPSL and CEACTEMA, Scientific and Technological Campus, University of Jaen, 23700 Linares, Spain; jmartine@ujaen.es

* Correspondence: chidalgo@ujaen.es

Abstract: The abandoned mining district of Linares (South Spain) is marked with waste from the mining and the processing of metal ores that pose an environmental hazard to watercourses. A combined analysis of waste, sediments and water was carried out to analyse the impact of a smelter on Baños Creek. The composition of the facility waste was determined using X-ray diffractometry and scanning electron microscopy. The total contents of the metal(loid)s in the waters and sediments of the watercourse were analysed, and sequential metal(loid) extraction of solid samples was carried out. The facility wastes consisted mainly of secondary minerals, such as natropharmacosiderite and spertiniite, as well as rare metal salts, such as mopungite and $\text{NaPb}_2(\text{CO}_3)_2(\text{OH})$. The leachates generated by these wastes were highly alkaline, with a pH of 10 and a total dissolved solids concentration of approximately 9 g L^{-1} . This Na-bicarbonate-type water had an As concentration above 200 mg L^{-1} and elevated levels of Pb, Sb and Zn ($5029 \text{ } \mu\text{g L}^{-1}$, $841 \text{ } \mu\text{g L}^{-1}$ and $525 \text{ } \mu\text{g L}^{-1}$, respectively). This highly contaminated lixiviate had a significant effect on the chemical quality of the waters and the bioavailability of metal(loid)s in the creek sediments, especially in the headwaters. In this zone, the As, Pb, Sb and Zn concentrations in the most mobile fraction of the sediments reached 1035 mg kg^{-1} , 261 mg kg^{-1} , 45 mg kg^{-1} and 30 mg kg^{-1} , respectively. By comparison, smelter slag and mining waste have a much lower impact on the waters and the mobile fraction of the sediments, while significantly increasing the total concentration of these potentially toxic elements in creek sediments.

Keywords: smelter; mining wastes; riverine environments; bioavailability; trace metal(oid)s



Citation: Cortada, U.; Hidalgo, M.C.; Martínez, J.; de la Torre, M.J. Mobility and Bioavailability of Metal(loid)s in a Fluvial System Affected by the Mining and Industrial Processing of Pb. *Geosciences* **2021**, *11*, 167. <https://doi.org/10.3390/geosciences11040167>

Academic Editors: Jesus Martinez-Frias and Javier Lillo

Received: 28 February 2021

Accepted: 4 April 2021

Published: 6 April 2021

Publisher's Note: MDPI stays neutral with regard to jurisdictional claims in published maps and institutional affiliations.



Copyright: © 2021 by the authors. Licensee MDPI, Basel, Switzerland. This article is an open access article distributed under the terms and conditions of the Creative Commons Attribution (CC BY) license (<https://creativecommons.org/licenses/by/4.0/>).

1. Introduction

Metal mining and the associated industries are one of the main sources of metal(loid) emissions worldwide [1–5], largely because of the enormous quantity of waste generated during metal smelting and the elevated concentrations of potentially toxic metal(loid)s, such as As and Pb, which are produced by refining processes [6–9]. Some of these materials are released into the atmosphere as fine particles, whereas liquid wastes and larger solid materials are deposited in the vicinity of mining operations [10–12]. The metal(loid)s can subsequently be dispersed through runoff and the chemical or biological conversion of the waste itself [13,14]. A large portion of these mobilised elements upon infiltration through soil can reach aquifers or be carried into surrounding river channels [15,16]. Thus, metal(loid)s can disperse over long distances, even reaching 400 km downstream from the source of contamination [17].

The impact of mining, mineral extraction or metallurgical wastes on the dispersion of the metal(loid)s are determined by numerous factors, such as the mineral composition and leaching potential, physicochemical environmental conditions, dispersion mechanisms of the trace elements and characteristics of the metal(loid)s themselves, depending on

the chemical form involved. Numerous studies have been conducted on this complex metal(loid) dispersion in recent years. Particularly notable are studies on the mineralogy and leaching potential of different types of smelter waste [18–20], as well as a review of the latest studies on the composition and potential environmental impact of slags [21]. They revealed a remarkably large heterogeneity in metallurgical wastes in terms of the variety of trace elements and mineralogical composition.

Upon reaching river courses, the mobility of dissolved metal(loid)s is influenced by the different physicochemical characteristics of the water, as different studies have shown for streams affected by mine drainage [22,23]. These outflows play an important role in the dispersion of metal(loid)s because elements can be easily stored in the sediments or remobilised downstream [24–26]. An in-depth understanding of the processes that influence metal(loid) mobilisation, distribution and bioavailability is vitally important to determine the potential risk of waste generated by extractive activity, mining and metallurgical facilities. Downstream spatial patterns in metal(loid)s from point sources are influenced by the dilution, storage and remobilisation of sediment in the channel and floodplain, hydraulic sorting, biological uptake and geochemical processes. The present study focused on the geochemical processes affecting both the spatial distribution of the contaminants and their bioavailability, as well as how different waste materials influenced the downstream spatial patterns of the metal(loid) concentrations, mobility and bioavailability.

The study was carried out in the middle and upper Baños Creek, within the mining district of Linares-La Carolina (Spain). The results of previous studies on this region have shown numerous remains of Pb mining and metallurgical industries along the creek banks, especially around the La Cruz smelter and the associated mining complex [27–29]. These mining industries were active during the 19th and 20th centuries and generated a large quantity of waste with significant metal and semimetal contents. These materials have enriched the trace elements in creek channel sediments and the floodplain [29]. The dispersal of these elements was connected with the atmospheric release of solid particles from mining waste deposits and the drainage of alkali leachates from inside the smelter. However, only the total metal(loid) content in the stream sediments was analysed. Similarly, the slag composition of the La Cruz smelter [30] did not explain the characteristics of the leachates that drained into the channel.

This oversight was addressed in this study by analysing different processes that affected the distribution of the metal(loid)s associated with the Pb industry along Baños Creek. The mobility and bioavailability of trace elements in the sediments and waters of the drainage network were studied. The impacts of different types of mining and metallurgical waste in the creek were investigated, considering both the mineral composition and the chemical form of the metal(loid)s present in the different types of smelter wastes.

2. Materials and Methods

2.1. Study Area

The study area was located 2 km north of the Linares (Spain) urban centre, which is the main municipality of the mining district of Linares–La Carolina and currently has 60,000 inhabitants. This region of the southern Iberian Peninsula has a continental Mediterranean climate and is characterised by dry and very hot summers, with an average annual precipitation of 650 L m^{-2} and average temperatures ranging between $7.2 \text{ }^\circ\text{C}$ in February and $28 \text{ }^\circ\text{C}$ in August. The seasonal rainy regime results in drying third-order channels for much of the year, as exemplified by the 13-km-long Baños Creek that runs through the study area (Figure 1).

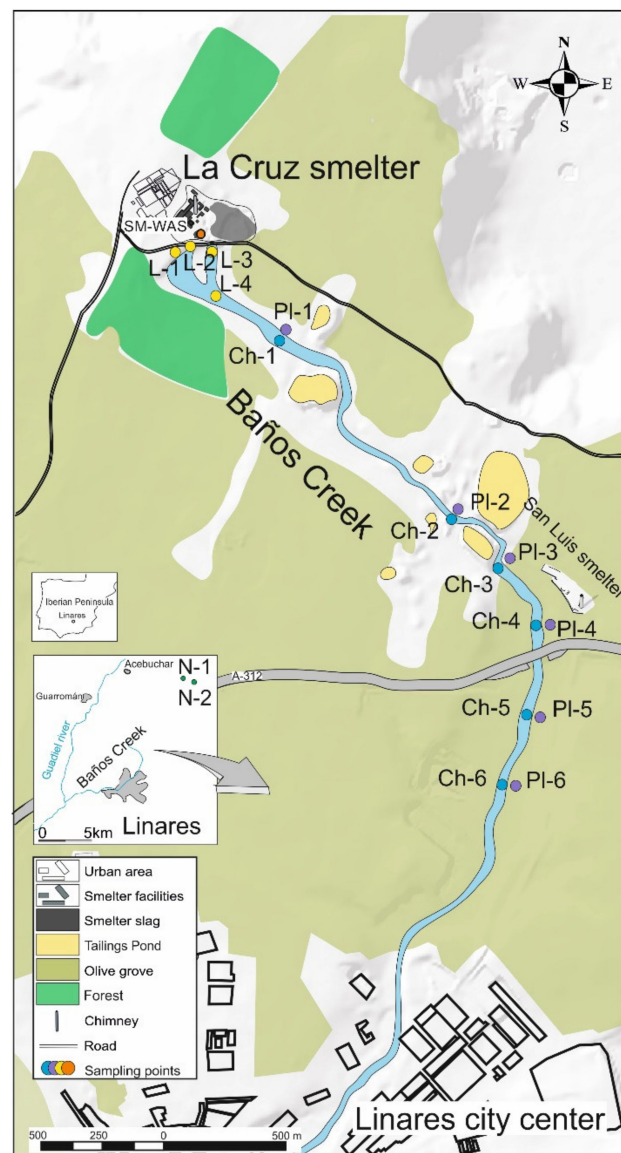


Figure 1. Study area and location of the sampling points: SM-WAS, metallurgical waste; L, leachate discharge area; Ch, creek bed sediments; PI, floodplain sediments.

The regional geology is characterised by a basement of metamorphic rocks (Palaeozoic phyllites and quartzites) and a granitic intrusion. These materials are richly veined with galena (PbS), chalcopyrite (CuFeS_2), sphalerite (ZnS) and lead-silver (Pb-Ag) sulfoantimonides, resulting in underground mining in the district and the development of an important associated industry [31]. This basement is superposed by a sedimentary cover composed of Triassic sands and clays, through which Baños Creek flows.

Although the Pb and Ag operations in the region are known to date back to the pre-Roman era, the district only reached global importance during the 19th and 20th centuries.

The high Pb concentration (over 70% by mass of lead in the ore) made the region one of the main sites for Pb production in the world between 1880 and 1920 (144,000 t in 1918). However, the combination of the high cost of underground mining and Pb prices resulted in the decline and subsequent closure of mines in the late 1980s.

Today, the landscape of this district remains interspersed with innumerable mining remains, waste rock deposits and abandoned industries, against which the old La Cruz Smelter stands out. This facility is located at the head of Baños Creek and was operated between 1830 and 1986, where it was the last metallurgical industry to close in the region.

The smelter processed 65,000 t of mineral concentrate per year over 150 years to produce Pb ingots and, to a lesser extent, Ag, Cu and Zn ingots [32]. The facility opened a secondary battery recycling line during the 1970s and 1980s to maintain the production cycle after the closure of numerous mining operations in the district.

The facility encompassed a 112,700 m² area that was used for different industrial operations and slag storage (Figures 1 and 2). The waste material is composed of a matrix of amorphous Fe and Si oxides, with traces of native wüstite, Fe and Pb [30]. Elevated Pb and Cu contents (22,890 and 4235 mg kg⁻¹, respectively) have been detected in these wastes [33].

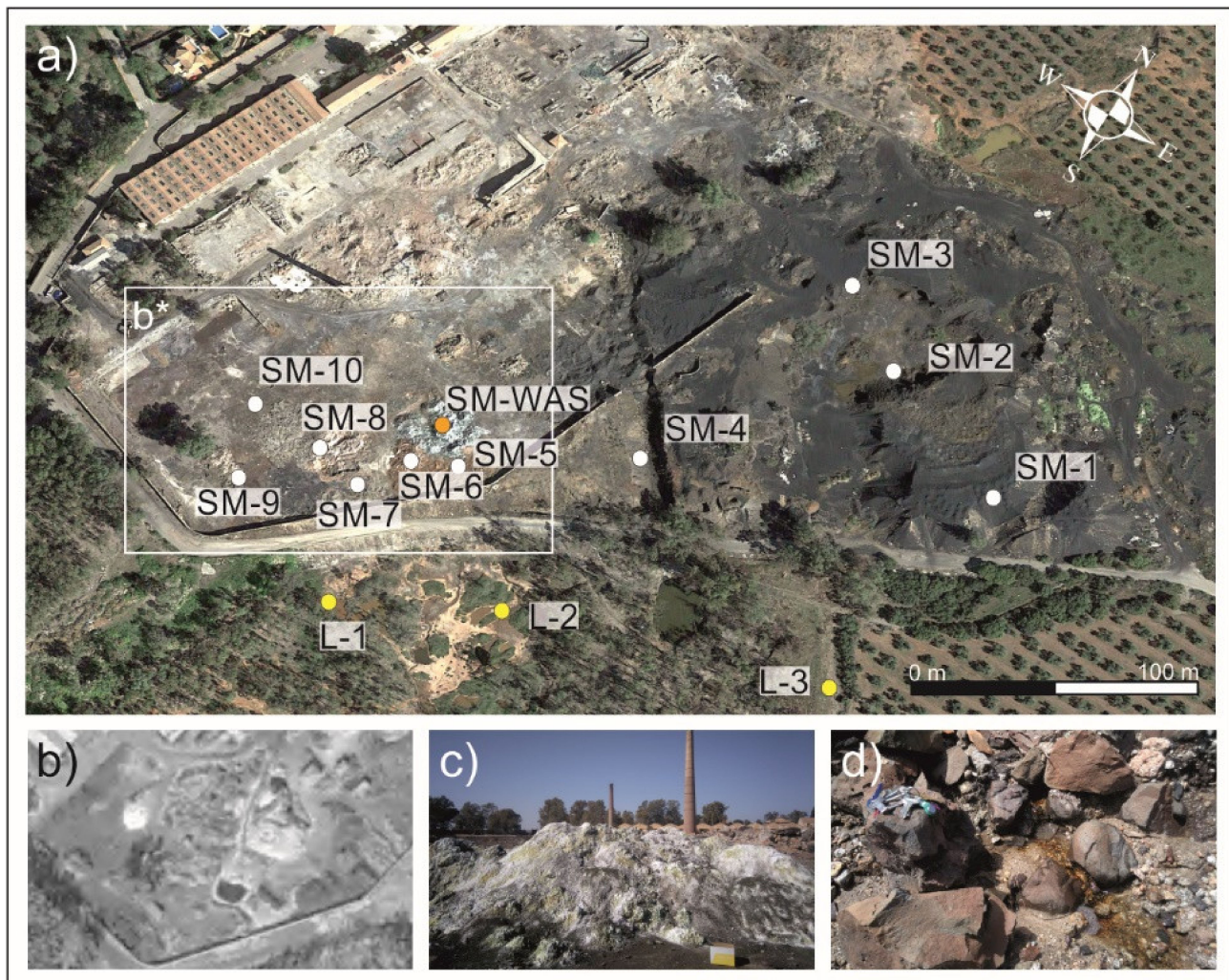


Figure 2. Images of the La Cruz smelter. (a) Aerial photograph of the facility (Google Earth, 2016) showing the location of different sampling points within and around the smelter. (b) Aerial photograph that was taken in 1984 of the area impacted by facility wastes. (c) Facility wastes (sample SM-WAS). (d) Leachate from the foot of the smelter.

The southwest zone of the smelter contains a settling pond for liquid waste, as well as various deposits of facility waste (Figure 2b,c). The alkaline leachates from these materials are still draining into the channel of Baños Creek. The sediments from this area at the headwaters of the creek have a pH of approximately 10 and very high contents of Sb (139 mg kg⁻¹), Zn (6263 mg kg⁻¹) and especially As (1921 mg kg⁻¹) [34].

The downstream end of the smelter contains old mine waste dumps and tailings ponds on both banks of Baños Creek. The waste dumps are composed of heterometric granitic materials produced by the re-deepening of shafts and galleries. The ponds are formed for waste material generated by the flotation recovery of galena (PbS) concentrate and have an

estimated total volume of 1,400,000 m³. The tailings' mineralogy is composed mainly of quartz, feldspar, calcite and ankerite, with traces of cerussite, lepidocrocite, melanterite and galena [35,36]. The Pb content (19,913 mg kg⁻¹) is elevated, of which, a high percentage occurs in bioavailable fractions, i.e., soluble and exchangeable fractions [37].

The San Luis smelter is located further downstream in the middle reach of the creek. San Luis was smaller than La Cruz (22,103 m² surface area, Figure 1) and was active for a shorter period (1890–1919). The wastes from this facility have been recovered for use in the cement industry, and the reclaimed land is currently used for agriculture.

2.2. Sampling and Geochemical Analysis

Two sampling campaigns were carried out. The first event was used to obtain La Cruz waste for physicochemical characterisation and included 11 sampling points for different deposits within the smelter (samples SM, Figure 2a). The pH, granulometry and total metal(loid) concentration were determined for each sample.

The second event comprised 18 sampling points (Figure 1), where the samples were used to analyse the chemical speciation of the metal(loid)s in the sediments of Baños Creek. Four sampling points were located at the head of Baños Creek (samples L) at the foot of the smelter deposits. The remaining sampling points were located downstream, both within the channel (samples Ch) and the floodplain (samples Pl). Reference samples were collected from the creek channel (N-1) and the floodplain (N-2) of La Atalaya Creek, 12 km NE of the smelter, from materials belonging to the same geological unit but that were free from mining or industrial impact. The pH, granulometry and total and fractionated metal(loid)s contents were determined for all the samples.

The samples were collected using a flighted screw Auger over the first 20 cm below the ground surface. Five subsamples were collected at each point at a 1 m cross-spacing and then mixed in a bag to obtain a total weight of 1.5 kg. The pH and granulometry of the samples were determined at the laboratories of the University of Jaen according to the UNE 10390:2012 and UNE 103101:1995 standards.

The samples were subsequently prepared for elemental analysis. Samples were screened using 2 mm PVC sieves and ground in an agate mortar. The screened samples were then sent to ALS Minerals (ISO 9002) in Vancouver (Canada) to determine the total and fractionated metal(loid)s contents. The samples were prepared for total content analysis using microwave-assisted multi-acid digestion [38]. This process consisted of placing the samples in a Teflon reactor together with a mixture of HNO₃, HClO₄ and HF, followed by microwave heating under high pressure. The resulting dry residue was dissolved in HCl and diluted with deionised water (Milli-Q 18.2 MΩ cm, Millipore Inc., Darmstadt, Germany).

Sequential extraction was carried out in four steps to detect the elements associated with the mobile (F1), exchangeable (F2), reducible (F3) and oxidisable (F4) fractions of the sediment. The F1 fraction was extracted by leaching the sample with deionised water. The F2 fraction was formed by cations adsorbed by clay and elements coprecipitated with carbonates and was extracted using a solution of ammonium acetate (C₂H₇NO₂) in acetic acid (CH₃COOH). The F3 fraction was composed of Fe and/or Mn oxides and hydroxides and extracted using an HCl-hydroxylamine solution (HCl-NH₂OH). The F4 fraction was formed by elements adsorbed by organic matter and/or sulfides and was extracted using a Na-pyrophosphate solution (Na₄P₂O₇). Finally, the residual fraction (F5) was obtained by subtracting the sum of F1, F2, F3 and F4 from the total concentrations of each sample.

The obtained solutions were analysed using inductively coupled plasma mass spectrometry (ICP-MS) to determine the total concentrations of Ag, Al, As, Ba, Be, Bi, Ca, Cd, Co, Cr, Cu, Fe, K, La, Mg, Mn, Mo, Na, Nb, Ni, P, Pb, Sb, Sc, Sn, Sr, Th, Ti, Tl, V, W, Y, Zn and Zr.

Inductively coupled plasma atomic spectrometry (ICP-AES) was used to analyse the samples for which the contents of Ag, As, Cu, Pb, Sb and Zn exceeded the maximum allowed by the ICP-MS analytical method (100 mg kg⁻¹ for Ag and 10,000 mg kg⁻¹ for

the other elements). The samples were analysed in duplicate as a quality control measure, and the study precision was evaluated using reference blanks and certified standards. The analytical method was validated by calculating the relative systematic error between the values obtained and those expected for the materials standards STD OREAS25A-4A and STD OREAS45E.

2.3. Mineralogical Analysis

The mineral composition of the facility wastes (SM-WAS) was analysed using X-ray powder diffraction (XRD) and scanning electron microscopy (SEM) at the laboratories of the Centre for Scientific and Technical Instrumentation (CICT) at the University of Jaen. The SM-WAS wastes were obtained at a depth of 20 cm and on the precipitate-covered surface (Figure 2c).

The XRD analyses were performed using a PANalytical X-ray diffractometer with CuK α radiation. The samples were prepared for analysis by grinding in an agate mortar to a grain size below 50 μm . The obtained diffractograms were analysed using HighScore Plus PANalytical software (version 4.6) and standard reference powder diffraction patterns.

For the SEM analysis, a high-resolution MERLIN (Carl Zeiss SMT AG) Field Emission Scanning Electron Microscope (FESEM) that allowed for obtaining secondary electron (SE) and retrodispersive electron (EBS) images was employed. The equipment has two detectors for the elemental microanalysis, an energy-dispersive X-ray spectroscopy detector (EDS) (Oxford Inca Energy 350X-MAX 50) and a WDS detector (Oxford Inca Wave 500). The samples were metalized with carbon to prepare them for the microanalysis.

2.4. Hydrochemical Analysis

Five locations were used for the water sampling along the drainage network: two points were located at the head of the creek (samples L-1 and L-4, Figure 1), one point was located upstream (sample Ch-1), and two points were located downstream (samples Ch-3 and Ch-6) of the area with waste dumps and tailings ponds (Figure 1). Sampling was carried out in November, during the wet season, just after a precipitation event that was intense enough to generate runoff along the investigated length of the creek.

The temperature, electrical conductivity (EC), pH and dissolved oxygen were measured in situ at each sampling point. Three subsamples were taken to determine the major and minor constituents, bicarbonate species and trace elements. All the samples were refrigerated until analysis. The subsample taken for trace element analysis was passed through a 0.45 μm filter and preserved with ultrapure nitric acid at pH < 2.5 to prevent the precipitation of metals and semimetals.

The analyses were performed at the CICT laboratories of the University of Jaen. The major and minor constituents were determined using ion chromatography (Metrohm Compact IC Flex), bicarbonates were determined using titration, and trace elements were analysed using ICP-MS (AGILENT model 7900 quadrupole ion filter).

The quality controls included the use of certified high-purity standards and reference blanks to verify the correct operation of the equipment, along with duplicate analyses.

3. Results and Discussion

3.1. Characterisation of the Smelter Wastes

The smelter slags (SM-1, 2, 3 and 4) had pHs of approximately 7, with low contents of As, Cu and Sb relative to the other wastes (Table 1). These samples consisted of Ca (7–12%) and Fe (11–24%) as the major elements, together with elevated contents of Pb (50,600 mg kg⁻¹ in SM-4) and Zn (41,600 mg kg⁻¹ in SM-3). This composition was similar to that obtained for Pb slags in other mining districts [8,14,39].

Table 1. Main physicochemical characteristics of the facility waste and slag obtained from the La Cruz smelter.

Heading	SM-1	SM-2	SM-3	SM-4	SM-5	SM-6	SM-7	SM-8	SM-9	SM-10	SM-WAS
pH	7	7	8	7	11	11	8	11	9	3	11
Silt (g kg ⁻¹)	17	0	10	15	55	40	10	25	35	25	40
Clay (g kg ⁻¹)	94	89	89	99	184	149	114	149	213	149	154
Elements (mg kg⁻¹)											
Ag	18	6	22	37	248	58	46	46	9	149	107
Al	36,800	39,000	35,600	65,300	28,700	40,100	35,600	29,700	84,800	4300	29,100
As	790	380	480	370	20,900	3070	680	7850	497	3410	29,700
Ba	275	400	290	3500	3060	3020	1390	1440	700	230	1600
Ca	109,800	122,500	117,500	70,700	31,700	47,100	72,600	47,400	31,000	1900	29,400
Cd	31	5	60	14	118	96	51	64	14	5	246
Co	115	65	103	59	66	51	57	43	32	131	493
Cr	50	35	48	938	105	116	30	129	65	36	65
Cu	3365	1800	3540	2140	7310	5730	2990	7440	402	13,550	46,900
Fe	204,250	236,000	236,000	113,500	42,700	65,800	52,100	55,900	20,500	389,000	124,500
K	11,150	11,700	9400	14,400	1100	2000	14,700	2900	2300	5200	2600
Mg	10,100	10,700	10,900	9500	4700	6100	11,900	7000	179,500	400	3700
Mn	2760	8300	4940	2090	751	925	3860	866	575	1380	10,150
Na	7300	4600	7500	2200	97,100	77,700	3000	86,100	800	2000	45,300
Ni	56	33	56	134	126	77	53	73	65	219	450
P	905	2190	1190	1030	230	180	650	300	280	120	1680
Pb	35,550	15,300	35,200	50,600	51,400	55,000	52,600	58,500	7010	50,800	71,200
S	16,800	9900	21,100	5100	7100	8800	9100	18,100	1300	64,100	8400
Sb	299	134	362	299	99,300	59,700	1405	69,500	515	786	41,600
Sn	525	170	270	80	1720	6760	230	9190	70	940	10,950
Ti	1750	1900	1600	2200	2500	1900	1200	1300	4500	400	1230
Tl	15	5	20	10	10	10	5	10	5	10	16
V	105	118	93	122	58	49	40	44	56	37	76
Zn	36,850	27,100	41,600	4120	17,700	52,400	5380	63,900	823	6960	59,400

The facility wastes (SM-6 to 10) did not have homogeneous compositions (Table 1). Samples SM-5, 6 and 8 had pH values above 10, with Na (8–10%) and Sb (6–10%) as the major elements and a high As content (3070 to 20,900 mg kg⁻¹). These samples also had significant levels of Pb (5–6%), Zn (2–6%) and Cd (64–118 mg kg⁻¹). In SM-10, however, the pH was approximately 3, and Fe (39%) and S (6%) were the major elements, probably from the oxidation of ferrous sulfides, such as pyrite (FeS₂). In addition, SM-10 had elevated concentrations of Pb (50,800 mg kg⁻¹), Cu (13,550 mg kg⁻¹) and, to a lesser extent, As (3410 mg kg⁻¹).

The SM-WAS deposits stood out at the centre of the study area because of their large size and visible alteration, manifesting as white, green and blue tones (Figure 2c). These wastes exhibited the highest contents of As (29,400 mg kg⁻¹), Cu (46,900 mg kg⁻¹) and Pb (71,200 mg kg⁻¹) over the entire area, along with elevated concentrations of Na (45,300 mg kg⁻¹) and Sb (41,600 mg kg⁻¹). The particles varied in size, the texture was mostly sandy fines, and the macroscopic colour was greyish brown. Given the unique composition of these wastes, a mineralogical analysis was carried out.

An XRD analysis produced complex mineralogical results for the SM-WAS sample (Figure 3a). The highest intensity peaks were associated with white rust (Fe(OH)₂), mopingite (NaSb(OH)₆), illite ((K,H₃O)(Al,Mg,Fe)₂(Si,Al)₄O₁₀[(OH)₂(H₂O)]) and quartz (SiO₂). Phases of natropharmacosiderite ((Na,K)Fe₄³⁺(AsO₄)₃(OH)₄·6–7H₂O) and franklinite ((Fe,Mn,Zn)²⁺(Fe,Mn)³⁺₂O₄) were also detected with lower-intensity peaks. To a lesser extent, oxides and hydroxides of As, Cu, Pb and Fe were observed, such as arsenolite (As₂O₃), spertiniite (Cu(OH)₂), minium (red lead) (Pb₃O₄) and goethite (α-Fe³⁺O(OH)), along with gypsum (CaSO₄·2H₂O) and calcite (CaCO₃). The slight elevation of the central section of the bottom curve of the diffractogram indicates the presence of poorly crystallised particles.

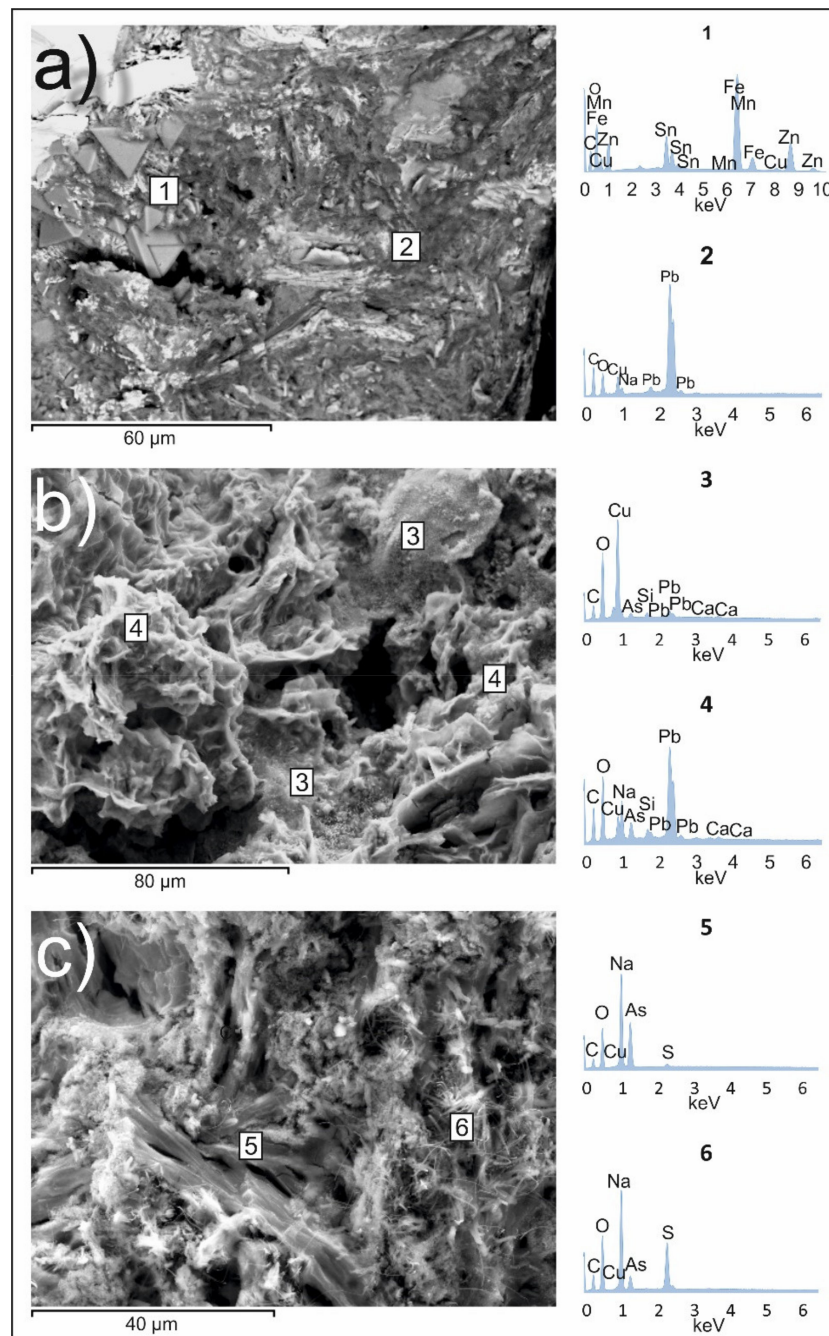


Figure 4. Scanning electron microscopy (SEM) images that were obtained by detecting the backscattered (a) and secondary (b,c) electrons. (1) Franklinite crystals; (2) vitreous matrix composed mainly of Na, Cu and Pb; (3) spertiniite aggregates; (4) NaPb₂(CO₃)₂(OH); (5) Na arsenate filaments; (6) thenardite precipitates.

The SEM data showed an atomic composition that was rich in Cu (9 wt%), Na (wt 4.6%), Pb (68 wt%) and O (18 wt%) (Figure 4, spectrum 2), which may imply a mineralogy that was based on small-grained oxides. Within this matrix, franklinite crystals (spectrum 1, Figure 4) containing Sn and Mn could be distinguished as atomic substitutes for Zn and Fe, respectively.

Figure 4b,c corresponds to the precipitates that partially covered the facility waste. Figure 4b shows spertiniite (spectrum 3, Figure 4) and NaPb₂(CO₃)₂(OH) phases (spectrum 4, Figure 4). These spectra show traces of As, Si, Pb and Ca in spertiniite and As, Ca and Cu

in the basic lead salt, indicating that these elements served as atomic substituents, as in the franklinite. Figure 4c shows that the thenardite precipitates (spectrum 6, Figure 4) were composed of Na, S and O, with trace levels of As and Cu. The same figure shows the Na arsenate filaments (spectrum 5, Figure 4) were a mineral phase that was not detected in the XRD analysis.

Therefore, the SM-WAS facility wastes were mainly composed of metal oxides and hydroxides that were associated with grains of quartz, illite and thenardite. The poorly crystallised grains were mainly composed of Cu, Na and Pb oxides. However, the SEM analysis revealed that the composition of the aforementioned mineral phases was not pure, with numerous atomic substitutions.

Elemental As is mainly associated with natropharmacosiderite and arsenolite. Natropharmacosiderite is a secondary mineral that is generated in neutral or basic pH environments with elevated As, Fe and Na levels [24]. Although exact data on the solubility of this mineral are not available [40], the pharmacosiderite group has been reported to be more stable in alkaline environments than other secondary phases of As, such as scorodite and arseniosiderite [40]. Arsenolite is a compound that is associated with nonferrous metallurgical activity that precipitates sublimated As in different smelting furnaces [41]. This compound also occurs as a secondary mineral in mining and industrial deposits with a high As content [42]. The arsenolite phase has high solubility and easily releases As into water [43]. The As precipitates as Na arsenate and is adsorbed by spertiniite, $\text{NaPb}_2(\text{CO}_3)_2(\text{OH})$ and thenardite, from which As can be easily mobilised.

Cu mainly occurs in spertiniite and forms oxides in poorly crystallised particles. Spertiniite is a mineral phase that redefines chrysocolla [44] and typically occurs as a secondary mineral in mining or smelting waste with a high Cu content. Spertiniite is moderately stable in alkaline environments [45].

Sb occurs in the form of mopungite, a very rare mineral phase that is found as an alteration of antimony sulfide. Mopungite is kinetically stable under ambient conditions and is generated in alkaline environments [46].

Pb forms minium, amorphous oxides and the basic Pb carbonate $\text{NaPb}_2(\text{CO}_3)_2(\text{OH})$. The last one is a rare secondary mineral [47] that is related to hydrocerussite ($\text{Pb}_3(\text{CO}_3)_2(\text{OH})_2$) [48], which has also been associated with the recycling of batteries for Pb extraction. Pb is a stable element at a pH of approximately 10 and is soluble under neutral or slightly acidic pH conditions [49].

Finally, Zn is associated with the mineral franklinite, which crystallises under conditions of high temperatures or pressures [50]. Franklinite was embedded in the poorly crystallised materials of the studied wastes. This compound is quite common in foundry slags with a high Zn content [8,18,51]. Franklinite is poorly soluble in alkaline environments, and Zn release is limited by the content of amorphous Fe oxides in the waste [52].

The aforementioned metal(loid)s, except for Zn, are associated with secondary phases related to the alteration of wastes under alkaline conditions. Some of these phases, such as arsenolite, mopungite or $\text{NaPb}_2(\text{CO}_3)_2(\text{OH})$, are not very stable and are easily soluble in water. Therefore, these materials can release metal(loid)s in the form of leachates. Considering the characteristics of the aforementioned phases, As and Sb are the most susceptible to mobilisation.

The composition of the facility waste differs from those of the slag (which is based on a matrix of amorphous Fe and Si oxides [30] and the mining waste, which mainly consists of quartz, feldspar, calcite and ankerite [35,36].

3.2. Geochemical Speciation

Table 2 shows the results obtained from the metal speciation according to the scheme in Section 2.2. The concentrations of As, Cd, Cu, Pb, Sb and Zn in the F1–F5 fractions of the Baños Creek sediments, the facility waste (SM-WAS) and the natural soil (La Atalaya Creek) are shown. The results for the slag from the La Cruz smelter and the Arrayanes tailings pond [37], near the PI-1 location, are also shown for comparison. These six elements were

selected because they are the most enriched by the mining, mineralurgical and metallurgical activities of the region [29,34,53,54].

Table 2. The As, Cd, Cu, Pb, Sb and Zn contents of the F1–F5 fractions of the Baños Creek sediments, facility waste (SM-WAS), natural soil, slag from the La Cruz smelter and a tailings pond near the creek. Max: maximum, Min: minimum, Std. Dev.: standard deviation.

		Stream Sediments				Max mg kg ⁻¹	%	Min mg kg ⁻¹	%	Std. Dev. mg kg ⁻¹	%	Facility Waste mg kg ⁻¹	%	Natural Soil mg kg ⁻¹		Slag mg kg ⁻¹		Tailings Pond mg kg ⁻¹	
		Mean mg kg ⁻¹	%	Median mg kg ⁻¹	%									mg kg ⁻¹	%	mg kg ⁻¹	%	mg kg ⁻¹	%
As	F1	107	27	0.3	0.5	1035	41	0.06	0.4	280	40	7250	24	0.3	2	<0.002	-	0.01	0.02
	F2	61	15	3	4	288	11	1.4	9	98	14	4320	15	0.5	4	51	17	1.2	3
	F3	102	26	19	32	533	21	4	28	149	21	9370	32	1.3	10	40	13	32	74
	F4	17	4	4	7	105	4	0.5	3	27	4	550	1.9	0.7	6	7	2	2	4
	F5	107	27	33	56	555	22	9	59	146	21	8210	28	10	78	204	67	8	19
Cd	F1	0.07	1.2	0.006	0.5	0.5	1.2	<0.002	-	0.1	1.1	0.6	0.2	<0.002	-	0.03	0.02	<0.002	-
	F2	3	52	0.5	50	20	49	0.07	45	6	49	106	43	0.01	23	0.9	3	0.4	21
	F3	2	26	0.2	24	11	27	0.02	14	3	28	73	30	0.01	19	0.6	74	0.06	35
	F4	0.02	0.3	0.01	0.6	0.1	0.3	<0.002	-	0.03	0.3	1.1	0.4	<0.002	-	0.5	4	0.09	27
	F5	1	20	0.3	26	9	22	0.06	41	2	21	65	26	0.03	58	29	19	1.2	70
Cu	F1	4	0.8	3	0.7	14	0.9	0.74	1.9	4	0.9	90	0.2	0.08	0.5	1.4	0.03	0.4	0.1
	F2	56	11	46	11	167	11	0.60	1.5	44	10	18,350	39	0.7	5	3	0.1	52	13
	F3	158	31	136	34	401	26	20	52	115	27	12,100	26	2	13	60	1.4	253	60
	F4	11	2	9	2	39	3	2	4	10	2	447	1.0	1	7	93	2	10	2
	F5	284	55	211	52	914	60	16	40	256	60	15,913	34	11	75	4077	96	103	25
Pb	F1	73	0.5	39	0.3	305	0.7	13	0.7	86	0.8	162	0.2	0.3	1.1	12	0.1	3	0.01
	F2	8961	61	7550	63	29	63	1195	63	7614	67	12,950	18	10	37	1188	5	5869	29
	F3	2918	20	2295	19	8110	18	290	15	1796	16	27,500	39	13	51	314	1.4	522	3
	F4	72	0.5	59	0.6	208	0.5	9	0.5	44	0.4	3990	6	0.7	3	1549	7	<0.002	-
	F5	2598	18	2098	17	8181	18	394	21	1799	16	26,598	37	2	8	19,827	87	13520	68
Sb	F1	4	6	0.5	1.4	45	21	0.08	0.7	11	19	2370	6	0.007	0.6	-	-	-	-
	F2	3	4	1.8	5	8	4	0.3	2	2	4	1325	3	0.004	0.4	-	-	-	-
	F3	5	7	4	11	10	5	0.7	6	3	5	1715	4	0.04	4	-	-	-	-
	F4	9	13	5	14	25	12	2	20	8	13	734	1.8	0.2	18	-	-	-	-
	F5	45	69	26	69	126	59	8	71	36	60	35,456	85	0.9	78	-	-	-	-
Zn	F1	6	0.6	0.7	0.3	30	0.5	0.1	0.2	10	0.6	160	0.3	0.1	0.3	12	0.02	0.1	0.05
	F2	208	20	34	13	2090	33	2	3	511	29	23,700	40	0.7	1.3	6369	12	12	6
	F3	475	45	120	47	2080	33	17	29	687	39	14,350	24	2	4	724	1.4	70	37
	F4	13	1.2	6	2	68	1.1	3	5	17	1	107	0.2	3	6	171	0.3	1.2	0.6
	F5	350	33	96	37	1998	32	38	63	537	30	21,083	35	47	89	44,005	86	107	56

The facility wastes (SM-WAS) had much higher elemental concentrations than the investigated soils and sediments. Among the analysed elements, As and, to a lesser extent, Sb were associated with the F1 fraction, whereas the remaining elements mostly occurred in F2, F3 and F5. The metal(loid)s were more associated with the more mobile soil fractions (F1, F2 and F3) in SM-WAS than in the slag, tailings ponds and natural soils. This result was consistent with SM-WAS composition of mainly highly soluble secondary minerals.

Figure 5 and Table 3 show the details of the distribution of the six selected metal(loid)s in the different fractions along Baños Creek.

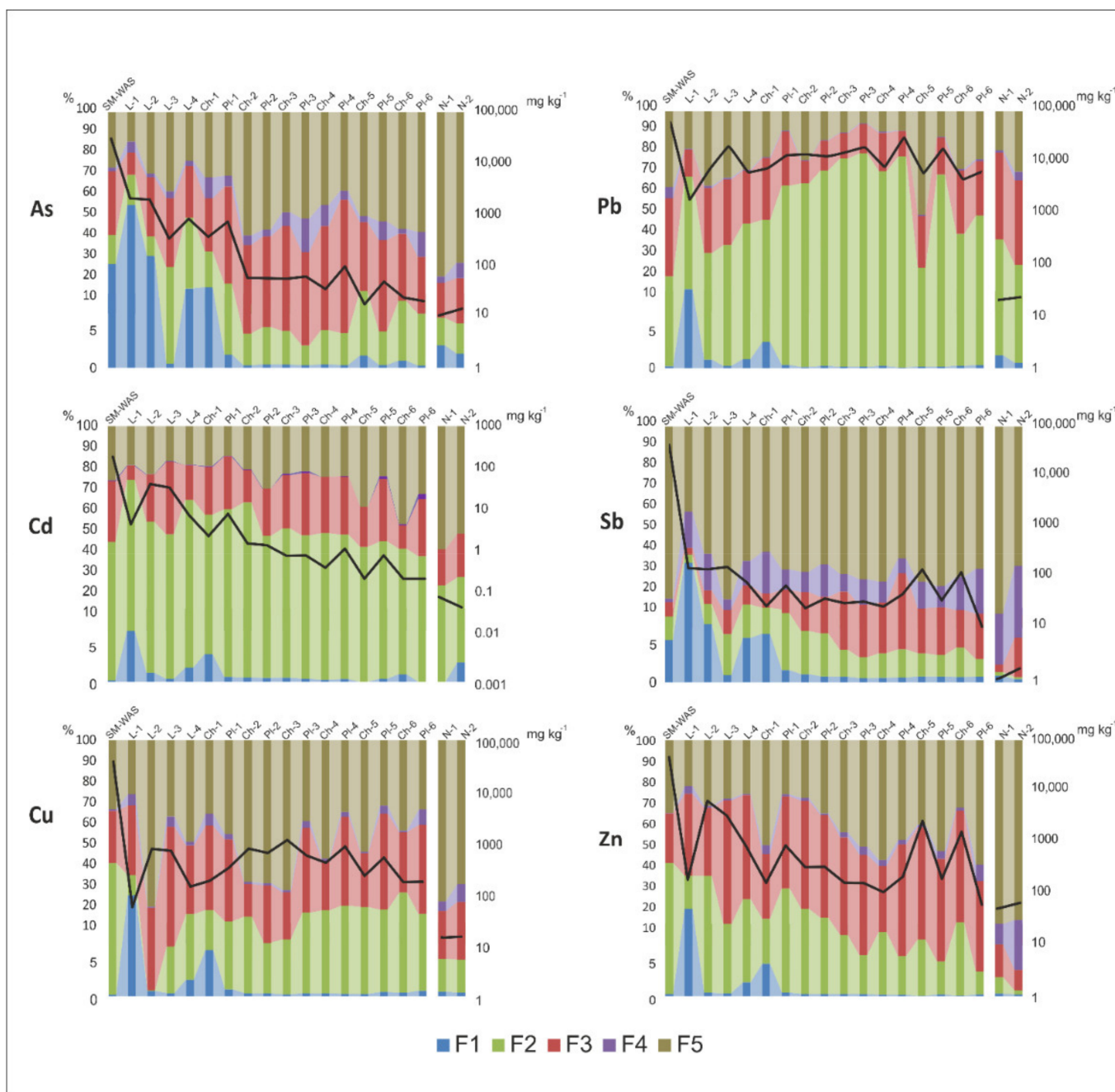


Figure 5. Graph showing the total (black line, in mg kg^{-1}) and fractional (F1, F2, F3, F4 and F5, in %) contents of As, Cd, Cu, Pb, Sb and Zn at the different sampling points.

Table 3. The pH, silt-clay content, fractional and total concentrations of As, Cd, Cu, Pb, Sb and Zn in the facility waste (SM-WAS), floodplain (PI-1 to PI-6) and channel (Ch-1 to Ch-6) of Baños Creek.

	SM-WAS	L-1	L-2	L-3	L-4	Ch-1	PI-1	Ch-2	PI-2	Ch-3	PI-3	Ch-4	PI-4	Ch-5	PI-5	Ch-6	PI-6	
pH	11.5	10.2	7.2	5.7	9.4	10.1	5.9	5.4	5.6	5.6	5.6	5.6	5.6	5.5	5.3	5.5	5.5	
Silt and clay (g kg ⁻¹)	184	590	361	814	193	466	660	236	123	412	433	108	638	29	510	18	403	
As	F-1 (%)	24	54	29	0.5	12	13	2	0.3	0.5	0.4	0.4	0.4	2	0.4	1.0	0.3	
	F-2 (%)	15	15	10	22	35	18	13	4	5	3	5	4	10	5	8	7	
	F-3 (%)	32	11	29	34	26	26	48	29	33	38	28	38	52	34	31	31	21
	F-4 (%)	2	5	2	3	2	10	5	5	3	7	17	11	5	3	9	2	12
	F-5 (%)	28	15	30	39	24	33	32	61	58	50	53	46	39	52	54	58	60
Total Conc. (mg kg ⁻¹)	29,700	1921	1824	319	774	345	683	55	56	53	59	34	93	17	47	23	20	
Cd	F-1 (%)	0.2	7	1.3	0.4	2	4	0.7	0.6	0.6	0.6	0.4	0.3	0.4	0	0.4	1.1	0.0
	F-2 (%)	43	67	52	47	62	53	59	62	46	49	46	47	41	43	39	36	36
	F-3 (%)	30	7	23	35	17	23	26	16	23	26	30	27	28	19	30	12	28
	F-4 (%)	0	0	0	0	0	0	0	0	0	1	1	0	0	0	1	1	3
	F-5 (%)	26	19	23	17	19	19	14	21	31	23	22	25	24	39	24	48	33
Total Conc. (mg kg ⁻¹)	246	4	39	32	7	2	7	1.4	1.2	0.7	0.7	0.4	1.0	0.2	0.7	0.2	0.2	
Cu	F-1 (%)	0.2	24	0.7	0.4	2	6	0.9	0.4	0.4	0.2	0.4	0.3	0.3	0.6	0.5	0.7	
	F-2 (%)	39	10	0	6	12	10	13	7	8	15	16	18	18	16	24	14	
	F-3 (%)	26	34	17	51	34	41	40	16	21	17	42	24	44	26	47	30	44
	F-4 (%)	1.0	6	0.5	5	2	6	3	1.0	0.9	0.9	3	1.3	2	0.7	4	0.9	8
	F-5 (%)	34	27	82	38	50	36	46	70	71	74	40	58	35	55	32	45	34
Total Conc. (mg kg ⁻¹)	46,900	59	829	754	149	194	354	831	683	1236	609	440	917	242	557	183	185	
Pb	F-1 (%)	0.2	12	1.1	0.3	1.2	3	0.4	0.1	0.3	0.2	0.2	0.1	0.2	0.2	0.3	0.4	
	F-2 (%)	18	56	29	34	43	43	63	64	71	77	79	70	78	22	69	39	48
	F-3 (%)	39	13	32	32	26	31	27	11	15	13	14	19	13	26	18	31	27
	F-4 (%)	6	0.4	1.0	0.8	0.6	0.6	0.4	0.3	0.3	0.3	0.4	0.5	0.3	0.8	0.5	0.9	0.8
	F-5 (%)	37	18	37	33	29	22	9	24	14	10	6	10	9	51	12	28	24
Total Conc. (mg kg ⁻¹)	71,200	2149	8761	25,013	7545	9027	16,785	17,090	15,376	18,365	23,879	9473	37,355	7077	22,446	5516	8080	
Sb	F-1 (%)	6	33	8	0.9	6	7	2	1.1	0.8	0.7	0.6	0.6	0.8	0.8	0.7	0.7	
	F-2 (%)	3	4	4	6	6	4	8	6	6	4	3	4	3	3	4	2	
	F-3 (%)	4	3	7	3	9	7	10	11	9	14	8	9	23	6	7	5	6
	F-4 (%)	2	18	5	12	21	10	10	16	9	13	10	8	13	11	16	20	
	F-5 (%)	85	42	63	86	67	62	71	72	68	73	76	77	65	77	79	74	71
Total Conc. (mg kg ⁻¹)	41,600	139	131	147	73	24	63	22	34	28	30	24	42	130	32	115	11	
Zn	F-1 (%)	0.3	18	0.4	0.4	2	4	0.5	0.3	0.3	0.3	0.2	0.2	0	0.2	0	0.2	
	F-2 (%)	40	16	33	10	21	8	27	18	13	8	5	9	8	5	11	3	
	F-3 (%)	24	40	33	61	51	32	45	53	50	44	38	30	44	50	37	54	28
	F-4 (%)	0.2	4	1.1	0.9	0.7	4	0.9	1.4	0.9	2	4	3	2	1.3	4	1.4	8
	F-5 (%)	35	22	32	28	26	51	26	28	36	45	52	58	49	41	54	33	61
Total Conc. (mg kg ⁻¹)	59,400	171	6263	3195	770	148	822	302	308	149	146	97	196	2514	178	1529	62	

The total As concentrations gradually decreased downstream from the sampling points at the head of the creek. The As concentration reached a maximum of 1921 mg kg⁻¹ in L-1 and a minimum of 17 mg kg⁻¹ in Ch-5 (Table 2). This latter value was similar to those obtained for the natural soils. The fractional analysis results for L-1 and L-2, which were affected by the leachate discharge from the facility waste, show that As mostly occurred in the most soluble fraction (F1), reaching 54% of the total content in L-1. In contrast, the As content in this fraction did not reach even 1% of the total concentration in L-3, which was obtained from the drainage channel in the perimeter of the slag deposit. This result indicates that As was less mobile in the smelter slag than in the facility wastes.

The percentage of the F1 fraction decreased with increasing distance from the leachate discharge zone, whereas the F3 fraction (associated with Fe and Mn oxides and hydroxides) and the residual fraction (F5) both increased.

A significant Cd contribution is detected from both the smelter slag (32 mg kg⁻¹ in L-3) and facility waste (39 mg kg⁻¹ in L-2), and the Cd content gradually decreased downstream. The Cd content was mainly associated with the exchangeable and bioavailable fraction along the investigated length of the creek, although the residual fraction increased with distance from the smelter. The presence of Cd in the exchangeable fraction largely resulted from the similarity between the cationic radii of Cd (0.97 Å) and Ca (0.99 Å), which favoured coprecipitation with carbonates and incorporation into the calcite mineral structure [55].

The total Cu concentration reached a maximum in Ch-3 from the lower reach of the channel and a minimum in L-1 from the discharge zone of leachates from the facility wastes. Therefore, the Cu distribution along the creek was very different from that of As and Cd, and would be related to the smelter slag and tailings ponds. Elemental Cu was mainly associated with Fe and/or Mn oxides and hydroxides and the residual fractions throughout the watercourse.

Pb mainly occurred in the exchangeable and bioavailable phase (F2). The highest Pb content was found in the vicinity of the smelter and the tailings ponds, similar to Cu. Around the tailings pond, Pb predominated in fraction F2, which represented up to 76% of

the total Pb (Pl-3, Table 3). This result may have occurred because the Pb from the tailings ponds had an affinity towards the carbonate phase.

In contrast, Sb was generally associated with the residual and oxidisable fractions, as well as being bound to sulfides and/or organic matter (Table 3, F4). The highest Sb content occurred at the head of the creek because of the influence of facility wastes and smelter slag. Sb was also elevated in the channel in the lower reach of the creek (Ch-5 and Ch-6), in the vicinity of the former San Luis smelter. The presence of Sb in the least mobile fraction of the soil has been reported in other mine sites [56]. Generally, it confirms the low mobility of Sb in areas that are affected by mining and metallurgy.

Finally, there was a remarkable Zn percentage in the exchangeable and bioavailable fraction at the foot of the facility wastes (33% in L-2), where the maximum total Zn content was also found (6263 mg kg^{-1}). Zn was mainly associated with Fe/Mn oxides and hydroxides, and with the residual fraction over the rest of the creek. The Zn content was also high at the foot of the smelter slags (L-3) and near the San Luis smelter (Ch-5 and Ch-6, Table 3).

These results indicate that the facility wastes, smelter slags and tailings ponds had significantly different effects on the creek sediments. In the facility wastes, As, Cd, Cu, Pb, Sb and Zn were associated with the most bioavailable fractions and were highly mobile, such that the leaching and drainage to the creek of these elements resulted in the dispersion of metals and semimetals associated with the most bioavailable highly mobile fraction, favouring their leaching and transfer to the creek. The most mobile element was As, where the F1 fraction represented more than 50% of the total concentration in L-1. In contrast, Cu and Pb had limited mobility in this alkaline medium.

3.3. Hydrochemistry

Table 4 shows the main physicochemical characteristics of the leachate from the La Cruz waste dump and the waters that flow in the Baños Creek. The maximum annual average (AA) values of the dissolved metal(loid) concentrations according to the European Union environmental quality standards (EQSs) for priority toxic elements in surface waters (Directive 2008/105/EC) are also shown.

At the foot of the La Cruz smelter, the leachates that drain into the creek (sample L-1) had a very alkaline pH of 10.4, a low oxidation–reduction potential (ORP) of approximately 50 mV and an electrical conductivity (EC) of $8864 \mu\text{S cm}^{-1}$, indicating a high degree of mineralisation in the waters. The influence of the leachates decreased with increasing distance along the channel from the smelter, where mixing with surface runoff significantly changed the water chemistry. At 250 m downstream of the facility (L-4), a pH of 9.5 was recorded, and the EC dropped to $2219 \mu\text{S cm}^{-1}$. Both the pH and EC of the creek waters decreased rapidly, where Ch-3 (sampled 2 km from the smelter) had a pH and EC of approximately 7.6 and $200 \mu\text{S cm}^{-1}$, respectively. This decrease was observed all the way downstream to Ch-6, approximately 3 km from the leachate runoff zone.

The Piper diagram in Figure 6 shows the characteristics of these waters. As the smelter wastes were uniquely rich in Na, the leachates had a high Na bicarbonate content with a high percentage of sulfates. L-1 had a high salinity with a total dissolved solids (TDS) concentration of approximately 9 g L^{-1} . These brackish waters gave rise to the formation of precipitates and salt crusts on the surrounding soils, mainly constituted by Ca-Na sulfates and carbonates, together with Na arsenates [36].

Table 4. Physicochemical characteristics of the surface waters. T, temperature; EC electrical conductivity; ORP, oxidation–reduction potential. The maximum allowable annual average (AA) values for the selected elements are shown. Contents exceeding the AAs are bolded.

	L-1	L-4	Ch-1	Ch-3	Ch-6
T (°C)	12	12	12	12	12
EC ($\mu\text{S cm}^{-1}$)	8864	2219	415	200	184
pH	10.4	9.3	8.1	7.8	7.6
ORP (mV)	50	160	170	170	170
Dissolved O ₂ (mg L^{-1})	10	8.7	9.5	9.5	9.5
mg L⁻¹					
Na ⁺	1864	505	65	5	2
K ⁺	41	19	7	5	4
Ca ²⁺	6	15	14	29	29
Mg ²⁺	2	7	3	3	3
Cl ⁻	31	19	9	3	2
SO ₄ ²⁻	1621	438	44	30	19
HCO ₃ ⁻	1696	751	152	75	80
CO ₃ ²⁻	862	104	0	0	0
$\mu\text{g L}^{-1}$					
As (50 $\mu\text{g L}^{-1}$ AA)	22,0676	31,890	530	5	6
Cd (0.1 $\mu\text{g L}^{-1}$ AA)	3	5	2	0.1	0.04
Cu (40 $\mu\text{g L}^{-1}$ AA)	313	434	64	47	55
Pb (7.2 $\mu\text{g L}^{-1}$ AA)	5029	787	337	132	125
Sb	841	487	28	1	2
Zn (300 $\mu\text{g L}^{-1}$ AA)	525	132	58	36	44

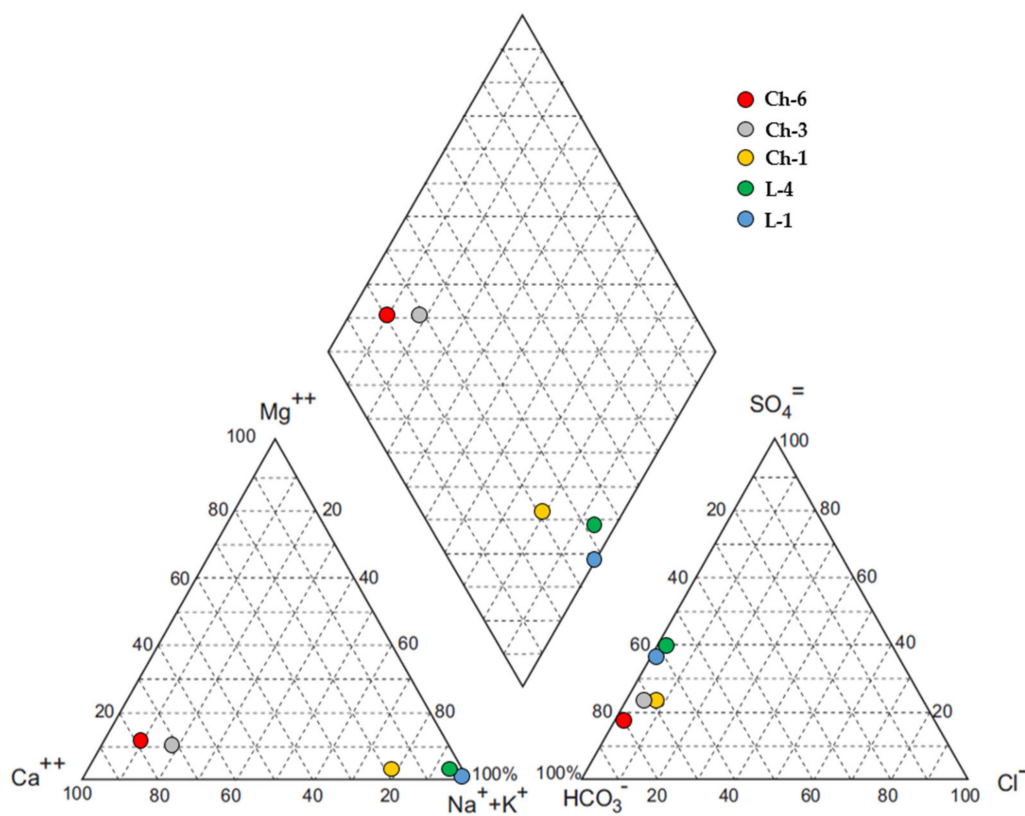


Figure 6. Piper diagram and hydrochemical types of the analysed water samples. L, leachates; Ch, surface waters.

Downstream, the water (Ch-3 and Ch-6) was predominantly of the Ca bicarbonate type, with low mineralisation, similar to that of other channels in this mining district [9,57,58]. However, the water in the headwater reach of the creek (Ch-1, Figure 6) was of the Na bicarbonate type, clearly reflecting the mixing between weakly mineralised natural water and the leachates from the smelter.

Table 4 also presents the concentrations of six dissolved metal(loid)s (As, Cd, Cu, Pb, Sb and Zn), which were chosen due to their high abundance and possible environmental effects. As expected, the maximum concentrations occurred in the leachates of the facility wastes (L-1), where very high contents were detected for Cu ($313 \mu\text{g L}^{-1}$), Pb ($5029 \mu\text{g L}^{-1}$), Sb ($841 \mu\text{g L}^{-1}$) and Zn ($525 \mu\text{g L}^{-1}$); the As content above 220 mg L^{-1} is especially alarming.

At 250 m downstream (L-4), there was a significant decrease in the contents of As, Pb, Sb and Zn, although the concentration of As remained very high at above 31 mg L^{-1} . Cd and Cu increased slightly; this could be attributed to the leachates from the smelter slag, which joined the creek waters at that point.

The contents of six elements decreased exponentially further downstream and stabilised beyond 2 km (Ch-3), where the highest dissolved metal concentrations corresponded to Cu ($47 \mu\text{g L}^{-1}$) and Pb ($132 \mu\text{g L}^{-1}$). This result may indicate that the source of these metals was the mining waste located between the sampling points for Ch-1 and Ch-3 (Figure 1).

The notable reduction in the mineralisation of the stream waters from the head of the creek indicated an important dilution resulting from the mixing of leachates with the natural waters. However, this process alone cannot be responsible for the marked decrease in the sulfate, carbonate, Na, As and Pb contents; further causes included the precipitation and coprecipitation processes of the sulfates and carbonates with Na and Pb, together with the presence of Na arsenates in the waste environment. Adsorption processes onto sediments and the coprecipitation and/or precipitation of metals and semimetals along the channels are common in mining environments [59,60]. This interpretation is consistent with the As and Pb speciation in sediments. Thus, the increase in the As and Pb contents in the floodplain sediments was linked to the exchangeable fractions (cations adsorbed by clay and elements coprecipitated with carbonates) and the reducible fractions.

The leachates generated from the facility wastes at the La Cruz smelter were the main source of metal(loid) runoff in the solution along Baños Creek. These wastes were less abundant than the slag and mining waste but considerably more soluble and released significant quantities of Cd, Cu, Pb, Sb, Zn and especially As.

Secondary minerals related to the alteration of the facility wastes (mainly arsenolite, mopungite and $\text{NaPb}_2(\text{CO}_3)_2(\text{OH})$) are not very stable and are easily solubilised upon contacting water [43]. The lixiviation of these mineral phases has a strong influence on the chemical quality of the waters and the bioavailability of metal(loid)s in creek sediments, especially in headwaters. In this area, the concentrations of As, Pb, Sb and Zn in the most mobile fraction of sediments reached values of 1035 mg kg^{-1} , 261 mg kg^{-1} , 45 mg kg^{-1} and 30 mg kg^{-1} , respectively. Considering these elevated contents, there is a risk of remobilisation of these elements from the sediment as a secondary source of contamination of surface water [24,41]. On the other hand, the smelter slag and mining waste had a much lower impact on the waters and the mobile fraction of the sediments, although they significantly increased the total concentrations of these potentially toxic elements in the creek sediments.

Considering the EQSs for As, Cd, Pb and Zn (Table 4), the results regarding the metal contents of the leachates released in the upper Baños Creek considerably exceeded the European regulations. The As, Cd and Zn contents were attenuated beyond the zone of mining influence to allowable levels, leaving only Cu and Pb with risk values in the middle and lower reaches of the creek.

4. Conclusions

Geochemical analyses were performed on the sediments and waters of Baños Creek and combined with a mineralogical characterisation of the facility wastes of the La Cruz smelter to reveal dispersal mechanisms of metal(loid)s for this watercourse. The results showed the high environmental impact of the different types of waste from this mining and metallurgical industry on the surrounding soils and waters.

The mineral composition of the facility wastes mainly included highly alterable secondary phases and metal salts, which facilitated the generation of alkali leachates with highly elevated levels of metal(loid)s. The materials that constituted the smelter slag and tailings ponds were also exposed to weathering but were less soluble. Thus, the reducible and residual fractions predominated in the sediments affected by the mobilisation of the potentially toxic elements from the slag deposits and tailings ponds. Therefore, the mobilisation and redistribution of metals and semimetals were mainly related to particle transport processes.

Three main sources of metals(oids) were identified and affected the watercourse differently. The facility wastes released large quantities of As, Cd, Cu, Pb, Sb and Zn into the water, where they were bounded in the most mobile fraction of the creek sediments. The alkaline conditions of the leachate, together with the high solubility of the minerals that contained As, facilitated the As release into the waters, resulting in its considerably high contents there.

The smelter slags contained large quantities of Cd, Cu, Pb, Sb and Zn in the exchangeable (F2), reducible (F3) and residual (F5) fractions of the sediments. However, the concentrations of these metal(loid)s in the waters and the soluble fraction of the creek sediments were considerably lower. Furthermore, the tailings ponds and dumps located downstream of the smelter resulted in significant Cu and Pb enrichment of the sediments and, to a lesser extent, the Baños Creek waters.

These results indicate that the elements leached from the facility wastes had the highest concentrations, mobility and impact on the creek water quality.

The case of the Baños Creek can be a reference for the other watercourses that are affected by Pb-sulphide extraction and reworking. The result obtained in this study can represent the environmental risk posed by this type of waste. In the specific case of facility waste, the high solubility and the enormous quantities of As mobilised in solution make it necessary to completely isolate such materials. They are major sources of pollution that hamper the attainment of the water quality targets established by the Water Framework Directive.

Author Contributions: Conceptualization, U.C., M.C.H. and J.M.; formal analysis, U.C. and M.J.d.l.T.; software, M.J.d.l.T.; investigation, U.C., M.C.H., J.M. and M.J.d.l.T.; writing—original draft preparation, U.C.; writing—review and editing, U.C., M.C.H., J.M. and M.J.d.l.T.; project administration, M.C.H. All authors have read and agreed to the published version of the manuscript.

Funding: This research was funded by the Spanish Ministry of Economy and Competitiveness, Project CGL2013-45485-R.

Institutional Review Board Statement: Not applicable.

Informed Consent Statement: Not applicable.

Data Availability Statement: The data presented in this study are contained within the article.

Conflicts of Interest: The authors declare no conflict of interest.

References

1. Han, F.X.; Su, Y.; Monts, D.L.; Plodinec, M.J.; Banin, A.; Triplett, G.E. Assessment of global industrial-age anthropogenic arsenic contamination. *Naturwissenschaften* **2003**, *90*, 395–401. [[CrossRef](#)] [[PubMed](#)]
2. Olías, M.; Cánovas, C.R.; Macías, F.; Basallote, M.D.; Nieto, J.M. The Evolution of Pollutant Concentrations in a River Severely Affected by Acid Mine Drainage: Río Tinto (SW Spain). *Minerals* **2020**, *10*, 598. [[CrossRef](#)]

3. Mayes, W.M.; Potter, H.A.B.; Jarvis, A.P. Inventory of aquatic contaminant flux arising from historical metal mining in England and Wales. *Sci. Total Environ.* **2010**, *408*, 3576–3583. [[CrossRef](#)] [[PubMed](#)]
4. Bundschuh, J.; Litter, M.I.; Parvez, F.; Román-Hoss, G.; Nicolli, H.B.; Jean, J.S.; Liu, C.W.; López, D.; Armienta, M.A.; Guilherme, L.R.G.; et al. One century of arsenic exposure in Latin America: A review of history and occurrence from 14 countries. *Sci. Total Environ.* **2012**, *429*, 2–35. [[CrossRef](#)]
5. Islam, M.S.; Ahmed, M.K.; Raknuzzaman, M.; Al Mamum, M.H.; Islam, M.K. Heavy metal pollution in surface water and sediment: A preliminary assessment of an urban river in a developing country. *Ecol. Indic.* **2015**, *48*, 282–291. [[CrossRef](#)]
6. Piatak, N.M.; Seal, R.R.; Hammarstrom, J.M. Mineralogical and geochemical controls on the release of trace elements from slag produced by base- and precious-metal smelting at abandoned mine sites. *Appl. Geochem.* **2004**, *19*, 1039–1064. [[CrossRef](#)]
7. Navarro, A.; Cardellach, E.; Mendoza, J.L.; Corbella, M.; Domenech, L.M. Metal mobilization from base-metal smelting slag dumps in Sierra Almagrera (Almería, Spain). *Appl. Geochem.* **2008**, *23*, 895–913. [[CrossRef](#)]
8. Andrade-Lima, L.R.P.; Bernardes, L.A. Characterization of the lead smelter slag in Santo Amaro, Bahia, Brazil. *J. Hazard. Mater.* **2011**, *189*, 692–699. [[CrossRef](#)]
9. Cortada, U.; Martínez, J.; Rey, J.; Hidalgo, M.C. Assessment of tailings pond seals using geophysical and hydrochemical techniques. *Eng. Geol.* **2017**, *223*, 59–70. [[CrossRef](#)]
10. Nriagu, J.O.; Pacyna, J.M. Quantitative assessment of worldwide contamination of air, water and soils by trace metals. *Nature* **1998**, *333*, 134–139. [[CrossRef](#)]
11. El Adnani, M.; Plante, P.; Benzaazoua, M.; Hakkou, H.; Bouzahzah, H. Tailings Weathering and Arsenic Mobility at the Abandoned Zgounder Silver Mine, Morocco. *Mine Water Environ.* **2016**, *35*, 508–524. [[CrossRef](#)]
12. Kříbek, B.; Majer, V.; Knésl, I.; Keder, J.; Mapani, V.; Kamona, F.; Mihaljevic, M.; Ettlér, V.; Penizek, V.; Vanek, A.; et al. Contamination of soil and grass in the Tsumeb smelter area, Namibia: Modeling of contaminants dispersion and ground geochemical verification. *Appl. Geochem.* **2015**, *64*, 1–17. [[CrossRef](#)]
13. Costagliola, P.; Benvenuti, M.; Chiarantini, L.; Bianchi, S.; Di Benedetto, F.; Paolieri, M.; Rossato, L. Impact of ancient metal smelting on arsenic pollution in the Pecora River Valley, Southern Tuscany, Italy. *Appl. Geochem.* **2008**, *23*, 1241–1259. [[CrossRef](#)]
14. Ettlér, V.; Johan, Z.; Kříbek, B.; Sebek, O.; Mihaljevic, M. Mineralogy and environmental stability of slags from the Tsumeb smelter, Namibia. *Appl. Geochem.* **2009**, *24*, 1–15. [[CrossRef](#)]
15. Domínguez, M.T.; Alegre, J.M.; Madejón, P.; Madejón, E.; Burgos, P.; Cabrera, F.; Marañón, T.; Murillo, J.M. River banks and channels as hotspots of soil pollution after large-scale remediation of a river basin. *Geoderma* **2016**, *261*, 133–140. [[CrossRef](#)]
16. Sindern, S.; Tremöhlen, M.; Dsikowitzky, L.; Gronen, L.; Schwarzbauer, J.; Siregar, T.; Ariyani, F.; Irianto, H.E. Heavy metals in river and coast sediments of the Jakarta Bay region (Indonesia)—Geogenic versus anthropogenic sources. *Mar. Pollut. Bull.* **2016**, *110*, 624–633. [[CrossRef](#)]
17. Veadó, M.V.; Arantes, I.A.; Oliveira, A.H.; Almeida, M.R.M.G.; Miguel, R.A.; Severo, M.I.; Cabaleiro, H.L. Metal Pollution in the Environment of Minas Gerais State—Brazil. *Environ. Monit. Assess.* **2006**, *117*, 157–172. [[CrossRef](#)]
18. Ettlér, V.; Legendre, O.; Bodéan, F.; Touray, J.C. Primary phases and natural weathering of old lead-zinc pyrometallurgical slag from Pacibram, Czech Republic. *Can. Mineral.* **2001**, *39*, 873–888. [[CrossRef](#)]
19. Ettlér, V.; Johan, Z.; Baronnet, A.; Jankovsky, F.; Gilles, C.; Mihaljevic, M.; Sebet, O.; Strnad, L.; Bezdicka, P. Mineralogy of air-pollution-control residues from a secondary lead smelter: Environmental implications. *Environ. Sci. Technol.* **2005**, *39*, 9309–9316. [[CrossRef](#)]
20. Ettlér, V.; Johan, Z.; Bezdicka, P.; Draek, M.; Sebek, O. Crystallization sequences in matte and speiss from primary lead metallurgy. *Eur. J. Mineral.* **2009**, *21*, 837–854. [[CrossRef](#)]
21. Piatak, N.M.; Parsons, M.B.; Seal, R.R. Characteristics and environmental aspects of slag: A review. *Appl. Geochem.* **2015**, *57*, 236–266. [[CrossRef](#)]
22. Kovács, E.; Tamás, J.; Frančičković-Bilinski, S.; Bilinski, H. Geochemical study of surface water and sediment at the abandoned Pb-Zn mining site at Gyöngyösoroszi, Hungary. *Fresenius Environ. Bull.* **2012**, *21*, 1212–1217.
23. Omanović, D.; Pižeta, I.; Vukosav, P.; Kovács, E.; Frančičković-Bilinski, S.; Tamas, J. Assessing element distribution and speciation in a stream at abandoned Pb–Zn mining site by combining classical, in-situ DGT and modelling approaches. *Sci. Total Environ.* **2015**, *511*, 423–434. [[CrossRef](#)]
24. Haffert, L.; Craw, D.; Pope, J. Climatic and compositional controls on secondary arsenic mineral formation in high-arsenic mine wastes, South Island, New Zealand. *N. Zeal. J. Geol. Geophys.* **2010**, *53*, 91–101. [[CrossRef](#)]
25. Grosbois, C.; Meybeck, M.; Lestel, L.; Lefèvre, I.; Moatar, F. Severe and contrasted polymetallic contamination patterns (1900–2009) in the Loire River sediments (France). *Sci. Total Environ.* **2012**, *435–436*, 290–305. [[CrossRef](#)]
26. Petta, R.A.; Sindern, S.; Souza, R.F.; Campos, T.F.C. Influence of mining activity on the downstream sediments of scheelite mines in Currais Novos (NE Brazil). *Environ. Earth Sci.* **2014**, *72*, 1843–1852. [[CrossRef](#)]
27. Martínez, J. Caracterización Geoquímica y Ambiental de los Suelos en el Sector Minero de Linares. Ph.D. Thesis, Universidad Politécnica de Madrid, Madrid, Spain, 2002.
28. Martínez, J.; Rey, J.; Hidalgo, M.C.; Luque, J.A. El georrádar como técnica de diagnóstico de presas mineras abandonadas. El distrito de Linares (Jaén, España). *Geogaceta* **2014**, *55*, 63–66.
29. Cortada, U.; Hidalgo, M.C.; Martínez, J.; Rey, J. Impact in soils caused by metal(loid)s in lead metallurgy. The case of La Cruz Smelter (Southern Spain). *J. Geochemical. Explor.* **2018**, *190*, 302–313. [[CrossRef](#)]

30. Sierra, C.; Martínez, J.; Menéndez-Aguado, J.M.; Afif, E.; Gallego, J.R. High intensity magnetic separation for the clean-up of a site polluted by lead metallurgy. *J. Hazard. Mater.* **2013**, *248–249*, 194–201. [[CrossRef](#)]
31. Lillo, F. Geology and Geochemistry of Linares-La Carolina Pb-ore Field (Southeastern Border of the Hesperian Massif). Ph.D. Thesis, University of Leeds, Leeds, UK, 1992.
32. Gutiérrez-Guzmán, F. *Las Minas de Linares. Apuntes Históricos*; Colegio Oficial de Ingenieros Técnicos de Minas de Linares: Linares, Spain, 1999.
33. Hidalgo, M.C.; Rojas, D.; Benavente, J.; Rey, J.; Martínez, J.; De la Torre, M.J. Contaminación de aguas y suelos en el entorno de una escombrera de fundición (Distrito Minero de Linares, Jaén). In Proceedings of the II Congreso Ibérico de las Aguas Subterráneas, Valencia, Spain, 8–10 September 2014.
34. Cortada, U.; Hidalgo, M.C.; Martínez, J.; Rey, J. Dispersion of metal(loid)s in fluvial sediments: An example from the Linares mining district (southern Spain). *Int. J. Environ. Sci. Technol.* **2019**, *16*, 469–484. [[CrossRef](#)]
35. De la Torre, M.J.; Campos, M.J.; Hidalgo, M.C. Estudio Mineralógico de las Escombreras en el Distrito Minero de La Carolina (Jaén, España). *Macla* **2010**, *13*, 213–214.
36. De la Torre, M.J.; Hidalgo, M.C.; Rey, J.; Martínez, J. Mineralogical characterization of tailing dams: Incidence of abandoned mining works on soil pollution (Linares, Jaén). *Geophys. Res. Abstr.* **2012**, *14*, 133357.
37. Rojas, D.; Benavente, J.; Hidalgo, M.C.; Rey, J.; Martínez, J. Contenido total y fraccionamiento de metales y semimetales en las escombreras del distrito minero de Linares-La Carolina (Jaén). *GeoTemas* **2012**, *13*, 1495–1498.
38. Rice, S. Super Trace 4-Acid Digestion & ICP-MS/AES Analysis, ALS Global. *Yilgarn Geochem. Semin.* **2017**, *1*, 1–20.
39. Morrison, A.L.; Swierczek, Z.; Gulson, B.L. Visualisation and quantification of heavy metal accessibility in smelter slags: The influence of morphology on availability. *Environ. Pollut.* **2016**, *210*, 271–281. [[CrossRef](#)]
40. Drahotka, P.; Filippi, M. Secondary arsenic minerals in the environment: A review. *Environ. Int.* **2009**, *35*, 1243–1255. [[CrossRef](#)]
41. Romero, F.M.; Villalobos, M.; Aguirre, R.; Gutiérrez, M.E. Solid-Phase Control on Lead Bioaccessibility in Smelter-Impacted Soils. *Arch. Environ. Contam. Toxicol.* **2008**, *55*, 566–575. [[CrossRef](#)]
42. Zhu, X.; Wang, R.; Lu, X.; Liu, H.; Li, J.; Ouyang, B.; Lu, J. Secondary minerals of weathered orpiment-realgar-bearing tailings in Shimen carbonate-type realgar mine, Changde, Central China. *Mineral. Petrol.* **2015**, *109*, 1–15. [[CrossRef](#)]
43. Nordstrom, D.; Zhu, X.; McCleskey, R.; Königsberger, L.C.; Königsberger, E. Geochemical modeling and thermodynamic properties of arsenic species. In *Arsenic Research and Global Sustainability: Proceedings of the Sixth International Congress on Arsenic in the Environment (As2016)*, Stockholm, Sweden, 19–23 June 2016; CRC Press: Stockholm, Sweden, 2016; p. 135.
44. Farges, F.; Benzerara, K.; Brown, G.E. Chrysocolla redefined as spertiniite. *AIP Conf. Proc.* **2007**, *882*, 223–225. [[CrossRef](#)]
45. Gade, B.; Pöllmann, H.; Heindl, A.; Westermann, H. Long-term behaviour and mineralogical reactions in hazardous waste landfills: A comparison of observation and geochemical modelling. *Environ. Geol.* **2001**, *40*, 248–256. [[CrossRef](#)]
46. Roper, A.J.; Leverett, P.; Murphy, T.D.; Williams, P.A. The stability of the rare sodium antimonate, brizziite, and its role in Sb mobility. *Mineral. Mag.* **2018**, *82*, 89–93. [[CrossRef](#)]
47. Ibáñez-Insa, J.; Elvira, J.J.; Llovet, X.; Pérez-Cano, J.; Oriols, N.; Busquets, M.; Hernández, S. Abellaite, NaPb₂(CO₃)₂(OH), a new supergene mineral from the Eureka mine, Lleida province, Catalonia, Spain. *Eur. J. Mineral.* **2017**, *29*, 915–922. [[CrossRef](#)]
48. Siidra, O.; Nekrasova, D.; Depmeier, W.; Chukanov, N.V.; Zaitsev, A.; Turner, R.W. Hydrocerussite-related minerals and materials: Structural principles, chemical variations and infrared spectroscopy. *Acta Crystallogr. Sect. B Struct. Sci. Cryst. Eng. Mater.* **2018**, *74*, 182–195. [[CrossRef](#)]
49. Taylor, P.; Lopata, V.J. Stability and solubility relationships between some solids in the system PbO–CO₂–H₂O. *Can. J. Chem.* **1984**, *62*, 395–402. [[CrossRef](#)]
50. Catlett, K.M.; Heil, D.M.; Lindsay, W.L.; Ebinger, M.H. Soil Chemical Properties Controlling Zinc Activity in 18 Colorado Soils. *Soil Sci. Soc. Am. J.* **2002**, *66*, 1182. [[CrossRef](#)]
51. Zhang, Y.; Yu, X.; Li, X. Zinc recovery from franklinite by sulphation roasting. *Hydrometallurgy* **2011**, *109*, 211–214. [[CrossRef](#)]
52. Lindsay, W.L. Chemical Equilibria in Soils. *Clays Clay Miner.* **1980**, *28*, 319. [[CrossRef](#)]
53. Martínez, J.; Llamas, J.; De Miguel, E.; Rey, J.; Hidalgo, M.C. Determination of the geochemical background in a metal mining site: Example of the mining district of Linares (South Spain). *J. Geochem. Explor.* **2007**, *94*, 19–29. [[CrossRef](#)]
54. Martínez, J.; Llamas, J.; De Miguel, E.; Rey, J.; Hidalgo, M.C. Soil contamination from urban and industrial activity: Example of the mining district of Linares (southern Spain). *Environ. Geol.* **2008**, *54*, 669–677. [[CrossRef](#)]
55. Ma, X.; Zuo, H.; Tian, M.; Zhang, L.; Meng, J.; Zhou, X.; Min, N.; Chang, X.; Liu, Y. Assessment of heavy metals contamination in sediments from three adjacent regions of the Yellow River using metal chemical fractions and multivariate analysis techniques. *Chemosphere* **2016**, *144*, 264–272. [[CrossRef](#)]
56. Wilson, N.J.; Craw, D.; Hunter, K. Antimony distribution and environmental mobility at an historic antimony smelter site, New Zealand. *Environ. Pollut.* **2004**, *129*, 257–266. [[CrossRef](#)]
57. Hidalgo, M.C.; Rey, J.; Benavente, J.; Martínez, J. Hydrogeochemistry of abandoned Pb sulphide mines: The mining district of La Carolina (southern Spain). *Environ. Earth Sci.* **2010**, *61*, 37–46. [[CrossRef](#)]
58. Hidalgo, M.C.; Rey, J.; Martínez, J.; Benavente, J. Impact of abandoned mining works on surface water. *Int. Multidiscip. Sci. Geconf. SGEM* **2012**, *2*, 903.

-
59. Jain, C.K.; Ram, D. Adsorption of lead and zinc on bed sediments of the river Kali. *Water Res.* **1997**, *31*, 154–162. [[CrossRef](#)]
 60. Palmer, S.C.J.; van Hinsberg, V.J.; McKenzie, J.M.; Yee, S. Characterization of acid river dilution and associated trace element behavior through hydrogeochemical modeling: A case study of the Banyu Pahit River in East Java, Indonesia. *Appl. Geochem.* **2011**, *26*, 1802–1810. [[CrossRef](#)]